1-1-2011

Nonlinear time dependence of dark current in Charge-Coupled Devices

Justin Charles Dunlap
Portland State University

Erik Bodegom
Portland State University

Ralf Widenhorn
Portland State University

Citation Details

Justin C. Dunlap; Erik Bodegom; Ralf Widenhorn; Nonlinear time dependence of dark current in charge-coupled devices. Proc. SPIE 7875, Sensors, Cameras, and Systems for Industrial, Scientific, and Consumer Applications XII, 78750H (2011).

Nonlinear time dependence of dark current in Charge-Coupled Devices

Justin C. Dunlap, Erik Bodegom, and Ralf Widenhorn*
Portland State, Portland, OR 97207

ABSTRACT

It is generally assumed that charge-coupled device (CCD) imagers produce a linear response of dark current versus exposure time except near saturation. We found a large number of pixels with nonlinear dark current response to exposure time to be present in two scientific CCD imagers. These pixels are found to exhibit distinguishable behavior with other analogous pixels and therefore can be characterized in groupings. Data from two Kodak CCD sensors are presented for exposure times from a few seconds up to two hours. Linear behavior is traditionally taken for granted when carrying out dark current correction and as a result, pixels with nonlinear behavior will be corrected inaccurately.

Keywords: Dark current, image correction, digital imagers, CCD, exposure time non-linearity, impurities

1. INTRODUCTION

At the heart of a digital imager often sits a silicon CCD (Charge-Coupled Device) sensor. In the absence of light, electrons can be thermally excited from the valence to the conduction band of the silicon. The temperature dependence of dark current has been thoroughly studied.[1]-[4] The dark count signal depends approximately exponentially on the temperature.[5] Depending on the chip design, the surface, depletion, and diffusion dark current can contribute in varying amounts to the total dark current. Their contribution can be distinguished, for example, by their characteristic activation energy. The characteristic activation energy is half the band gap of silicon for the depletion current, and is equal to the band gap of silicon for the surface and diffusion current.[6]-[10] Not all pixels produce the same amount of dark current. So called hot pixels, pixels with an unusual high dark count, are distributed seemingly randomly across a CCD chip. The high dark count of the hot pixels is caused by impurities in the silicon. Such impurities can be lattice defects, or foreign atoms (e.g. Fe, Ni, and Au).[1]-[5]

In order to minimize dark current, scientific imagers are often cooled. One can correct for dark current by subtracting an image, taken with a closed shutter, from the light image. To get an accurate reflection of the dark current one needs to take the dark image under the same condition as the light image. The generation of dark current is a statistical process described by the Poisson distribution. Taking multiple dark frames under the same condition, and averaging the frames to create a master frame, improves the signal-to-noise ratio. Obtaining such a master dark frame can be time consuming but often leads to a significantly improved noise correction. Master dark frames can, in principle, be reused if the temperature and exposure time are unchanged. We have shown that dark frames can also be computed for any temperature after an initial calibration of the imager.[6]

It is generally assumed that the dark count increases linearly with exposure time. In principle this allows dark frames to be scaled to different exposure times. To do this, the bias offset, *Bias*, is subtracted and the thermal signal is obtained. To obtain a dark frame for a different exposure time, the thermal signal is scaled by a factor corresponding to the desired exposure time. The bias offset can then be added back to the scaled thermal signal to obtain the final scaled dark frame for the new exposure time. For example a 60 s dark frame, D_{60}, can be obtained from a 600 s frame, D_{600}, by calculating:

$$D_{60} = {}^{1}/_{10} * (D_{600} - Bias) + Bias \quad (1)$$

The advantage of a scaled dark frame is that a longer exposure frame provides a large signal-to-noise ratio; the scaling of that frame creates a short exposure frame which would have a larger signal-to-noise ratio than a frame taken at that exposure time. Fig. 1 shows the results obtained for scaled dark frames for two different cameras: The SBIG ST-8XE with a KAF-1602E CCD sensor and the Meade Pictor 416XT with a Kodak KAF-0400 CCD chip. The histograms of the count difference between a single 60 s dark frame and a master dark frame obtained from the average of ten 60 s

* ralfw@pdx.edu

Sensors, Cameras, and Systems for Industrial, Scientific, and Consumer Applications XII,
edited by Ralf Widenhorn, Valérie Nguyen, Proc. of SPIE-IS&T Electronic Imaging, SPIE Vol. 7875,
78750H · © 2011 SPIE-IS&T · CCC code: 0277-786X/11/$18 · doi: 10.1117/12.871962

exposures are shown in Fig. 1b. Ideally the distribution would show a single peak with all pixels having zero counts. Readout noise as well as dark current shot noise cause a widening of the distribution. The width of the distribution, as given by its standard deviation, is equal to 26.3 counts. In Fig. 1a, a 600 s frame is scaled to 60 s and subtracted from an individual 60 s frame. It took approximately the same camera time to obtain the scaled 60 s frame as it took to get the 60 s master frame. However, the scaled frame only requires one readout and should therefore have less readout noise. The histogram in Fig. 1a shows a long tail with many pixels having larger values for the individual frame than for the scaled frame. The resulting standard deviation has increased to 90.9 counts. The results for the Meade camera are similar and exhibit a poorer correction with the scaled frame (Fig. 1c) than for the master frame (Fig. 1d). Subtraction using the scaled frame shows a distinct second peak at approximately minus 350 counts in the resulting histogram. Hence, a group of pixels show a larger count when scaled from a long exposure frame.

For both cameras the result of the scaled dark frames is not quite as good as one would expect assuming a linear time dependence of the dark count. We found that the explanation of the poor correction of the scaled frame requires considering nonlinearities of the dark current versus exposure time. Such nonlinearities are well known when the count reaches values close to the full well of a pixel, however nonlinearities at lower signals have not been studied in detail. In this work we characterize the dark current of the two aforementioned sensors for different exposure times. We find that certain pixels exhibit a predictable nonlinear behavior. Furthermore, the nonlinear behavior of pixels can be categorized in groups with similar characteristics.

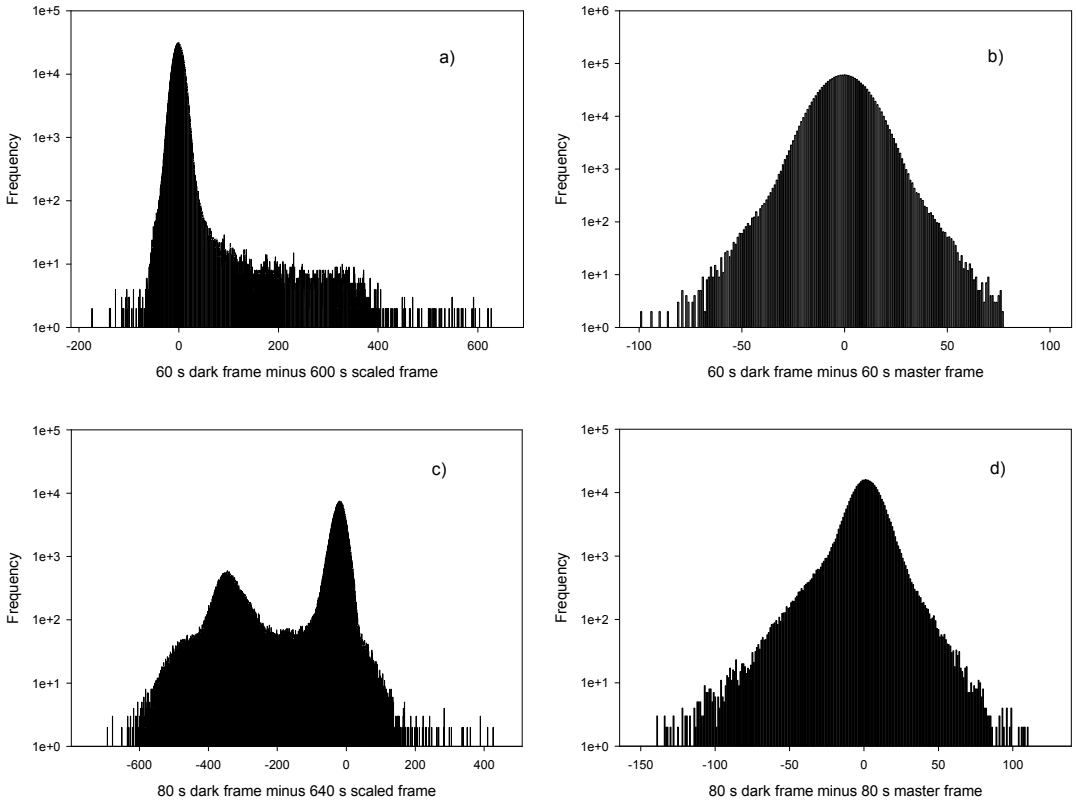

Fig. 1. Difference of an individual dark frame and a master frame, and the individual dark frame and a scaled dark frame. (a) Single 60 s frame minus an individual 600 s frame scaled to 60 s for the SBIG imager at T=288K.(b) Single 60 s frame minus the average of ten 60 s frames for the SBIG imager at T=288K. (c) Single 80 s frame minus a single 640 s frame scaled to 80 s for the Meade imager at T=278K. (d) Single 80 s frame minus the average of eight 80 s frames for the Meade imager at T=278K.

2. EXPERIMENTAL PROCEDURES AND RESULTS

2.1 SBIG ST-8XE

We obtained dark frames at 288 K for exposure times from 5 to 7,200 s. For exposure times smaller than 640 s the median pixel value of three frames was used. One frame was taken for exposure times of 900 s and above. Fig. 2a shows the dark current of 5 different pixels. The majority of pixels on the chip behave similarly to Pixel 4. The dark count is low and seems to increase linearly with exposure time. The other pixels show a larger dark count and would be considered to be hot pixels. The pixel with the highest dark count is Pixel 5. Its dark count increases approximately linearly up to 50,000 counts. This is actually slightly larger than the saturation count as listed by the manufacturer. Once a pixel has reached saturation, electrons start to bloom into neighboring pixels. Therefore, the dark count of a saturated pixel, as well as its neighbors, has to be considered with care. For exposure times shorter than about 100 s, the dark count of Pixel 2 is similar to the dark count of Pixel 5 (see Fig. 2b). However, whereas the dark signal increases linearly up to saturation for Pixel 5, Pixel 2 levels off much earlier. Pixel 3, while less hot than Pixel 2, also shows a decreasing slope versus exposure time.

This effect is even more dramatic for Pixel 1 as the dark count up to about 50 s is as high as the dark count of Pixel 5. For example at 40 s its dark count is 79 percent of the dark count of Pixel 5. However, at 7,200 s Pixel 1 has only 8 percent the dark count of Pixel 5. At 7,200 s, Pixel 1 generates dark current at the same rate as a regular pixel, as represented by Pixel 4. On the other hand, at low exposure times the pixel behaves more like a hot pixel. Using the dark count at short exposure times might therefore not always be a good measure of how a pixel behaves at long exposure times.

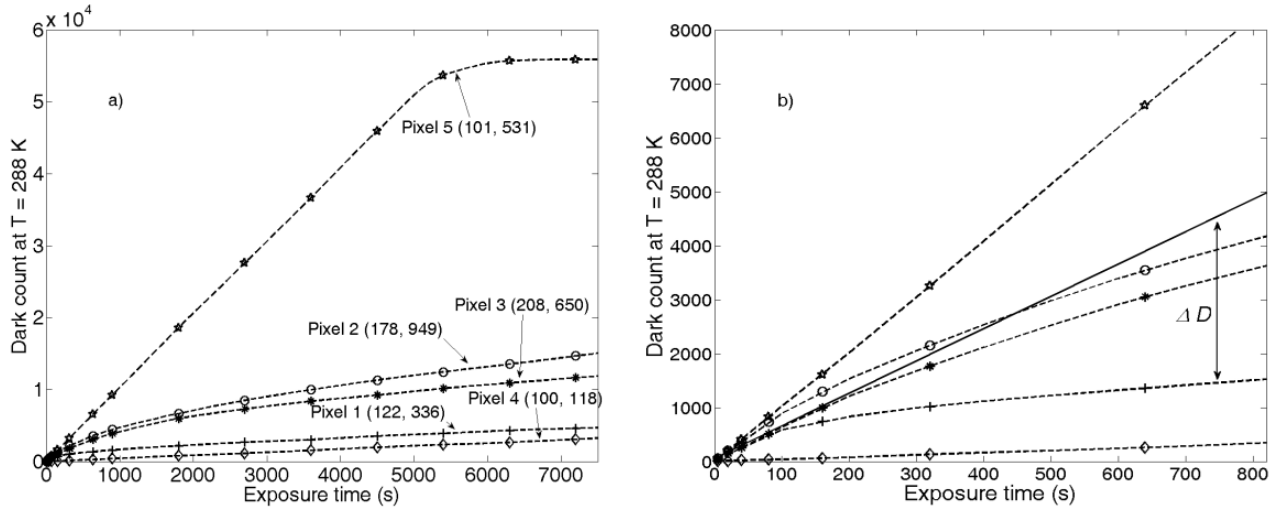

Fig. 2: Dark count at 288K as a function of exposure time for 5 pixels for the SBIG ST-8XE .
(a) Exposure times up to 7,200 s. (b) Enlargement with exposure times up to 800 s and linear fit to Pixel 1 (same pixels shown as in (a)).

To get a global overview of the linearity and nonlinearity of all pixels on the chip a linear fit of the type;

$$D_{fit} = bt \qquad (2)$$

was applied to dark frames from 5 s to 60 s (see solid line in Fig. 2b as the linear fit for Pixel 1). Hence, the parameter b represents the dark current in counts per second over this time interval. If it is assumed that the dark current is linear, the dark count can be calculated at any exposure time, t_0, as $D_{fit}(t_0)=bt_0$. One can conclude from Fig. 2 that this linear scaling to a different exposure time works well for pixels such as Pixel 4 and Pixel 5. However, for pixels such as Pixels 1, 2, and 3, which show a nonlinear dark current behavior, one predicts an incorrect value for the dark count. As seen in Fig. 2b, pixels that show a decreasing slope in the dark count versus exposure time plot will have an actual dark count that is lower than predicted by the fit. To evaluate the difference between the dark count obtained from the linear fit, D_{fit}, and the measured dark count, $D_{measured}$, we define:

$$\Delta D = D_{fit}(t_0) - D_{measured}(t_0) = b(t_0) - D_{measured}(t_0) \quad (3)$$

According to Eq (3) for Pixel 1 evaluated at t_0=160 s, ΔD is 295 counts. For a longer exposure time of t_0=640 s, this difference has increased to 2,778 counts.

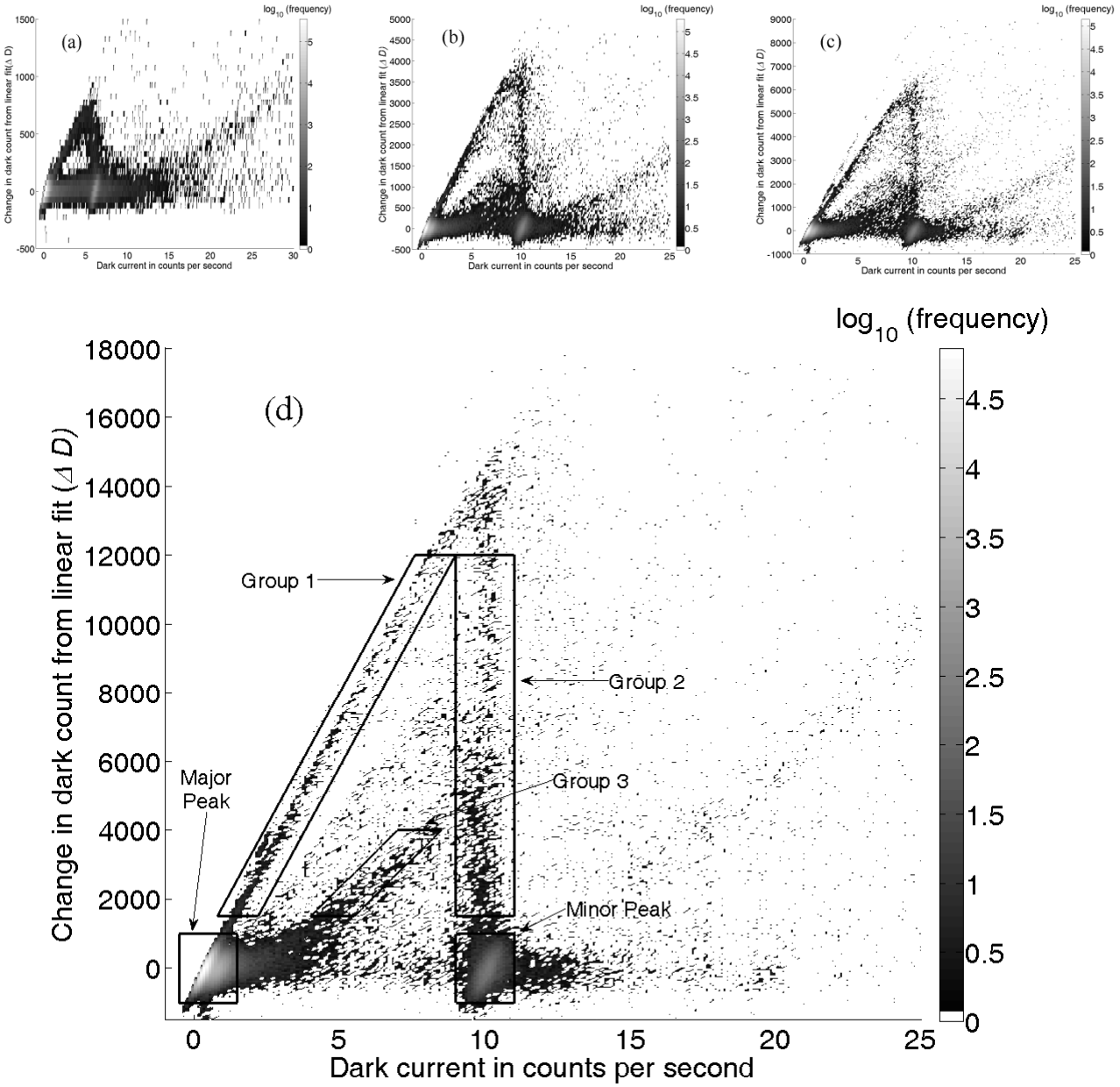

Fig. 3: Dark current from linear fit versus the change in dark count, ΔD, for the SBIG ST-8XE at 288 K evaluated at (a)320 s, (b)640 s, (c) 900 s, (d) 1,800 s.

Fig. 3 shows the distribution of the change in dark count, *ΔD,* at t_0=320 s (Fig. 3a), t_0=640 s (Fig. 3b), t_0=900 s (Fig. 3c), and t_0=1,800 s (Fig. 3d) versus the dark current which is given as the parameter *b* in Eq. (2) for exposure times from 5 to 60 s. For the figure the change in dark count vs. dark current plane is divided into areas of size 0.1 counts/s (dark current as given by the parameter *b* in Eq. 2) by 50 counts in the *y*-direction (*ΔD*).The number of pixels in each area, the

frequency, is then plotted. By far, the largest number of pixels is located in the Major Peak where approximately 1.5 million pixels (or 97 %) lie within the rectangle indicated in Fig. 3c. Another 17,000 pixels are in the Minor Peak with a dark current of approximately 10 counts/s and $\Delta D \approx 0$. Pixel 4 is an example of a pixel in the Major Peak while Pixel 5 is a Minor Peak pixel. Pixel 2, a typical Group 2 pixel, behaves like a Minor Peak pixel with a dark current of approximately 10 counts/s based on the linear fit. However, as one can see in Figs. 1 and 2, Group 2 pixels are nonlinear and have a lower dark count for larger exposure times. Pixels defined by Group 1 have a change in dark count which is approximately 5 times the dark count value at 1,800 s. For example, Pixel 1 has a dark count of 2,265 counts at 1,800 s, a predicted dark count based on a linear fit of 10,864 counts and hence a change in dark count of 8,599 counts. About 1,500 pixels are within the parallelogram identifying Group 1. Group 3 pixels, as represented by Pixel 3 in Fig. 1, also show a change in dark count, however their nonlinear behavior is smaller in magnitude. One also notices from Fig. 3 that a smaller number of pixels behave similarly to Group 3 pixels, but emerge from the Minor Peak rather than the Major Peak. Another distinct group of pixels could be identified in between Group 1 and Group 3. For clarity sake, we refrained from giving those pixels their own group designation. Other major distributions of pixels in Fig. 3 are pixels which are not located in the two peaks but, similar to the pixels in the peaks, have no significant change in dark count (i.e. $\Delta D \approx 0$). Finally, there are a number of pixels not shown in the graph that have a small dark current like Major Peak pixels and a negative change in dark count. We found that these pixels are located next to a hot pixel that saturated at longer exposure times, spilling electrons into neighboring pixels.

Grouping	**Approximate Pixel Count (1,560,600 total pixels)**
Major Peak	1,500,000
Minor Peak 1	17,000
Group 1	1,500
Group 2	2,500
Group 3	700

Table 1 -Pixel count of groups, as shown in Fig. 3(c), for the SBIG at an exposure time of 1,800s

2.2 Meade Pictor 416XT

From Fig. 1 we found that the KAF-0400 sensor in the Pictor 416XT camera, like the KAF-1602E sensor in the SBIG camera, shows a non-perfect correlation between a single dark frame and a scaled dark frame. Graphs similar to Fig. 3 were generated in order to find out if the sensor in the Meade camera also shows nonlinear dark current behavior that can be separated in distinct groups. Fig. 4 shows graphs with the dark current on the x-axis calculated from exposure times of 40 to 320 s at T=278 K. A linear fit of the dark count to those exposure times was applied and extrapolated to 640 s (Fig. 4a), 900 s (Fig. 4b), and 1,800 s (Fig. 4c). As in the previous section, the change in dark count, ΔD, is then calculated for each pixel and displayed on the y-axis. The shades of grey indicate how many pixels show a particular ΔD for a given dark current. Like in the graphs for the SBIG camera, Fig. 4 is divided in areas of 0.1 counts/s by 50 counts.

The different panels in Fig. 4 clearly show that the KAF-0400 chip shows distinct groups as well. As one increases the exposure time at which ΔD is evaluated, groupings become more distinct. We therefore used the largest exposure time of 1,800 s (Fig. 4c) to define the different groups as given in Table 2. Analogous to the SBIG camera, the Meade camera has groups similar to Group 1, Group 2, Major Peak, and Minor Peak as in Fig. 3. The Major Peak for the Meade contains approximately 324,000 pixels, corresponding to about 82.4% of the chip. Pixels in the Major Peak have low dark current and, unlike for the SBIG camera, a negative ΔD. Instead of a single Minor Peak, Fig. 4 shows two minor peaks that are also located at negative ΔD values. Minor Peak 1 is located at about 9 counts/s and Minor Peak 2 at about 18 counts/s. Group 1a and Group 2a mirror the characteristics of Group 1 and Group 2 in the SBIG camera. Group 1b and Group 2b share the same shape as Group 1a and Group 2a, but are shifted to the right. Group 1b emerges from the Minor Peak 1 and connects with Group 2b, pixels that have the same dark current as Minor Peak 2 pixels but with various changes in dark count ΔD.

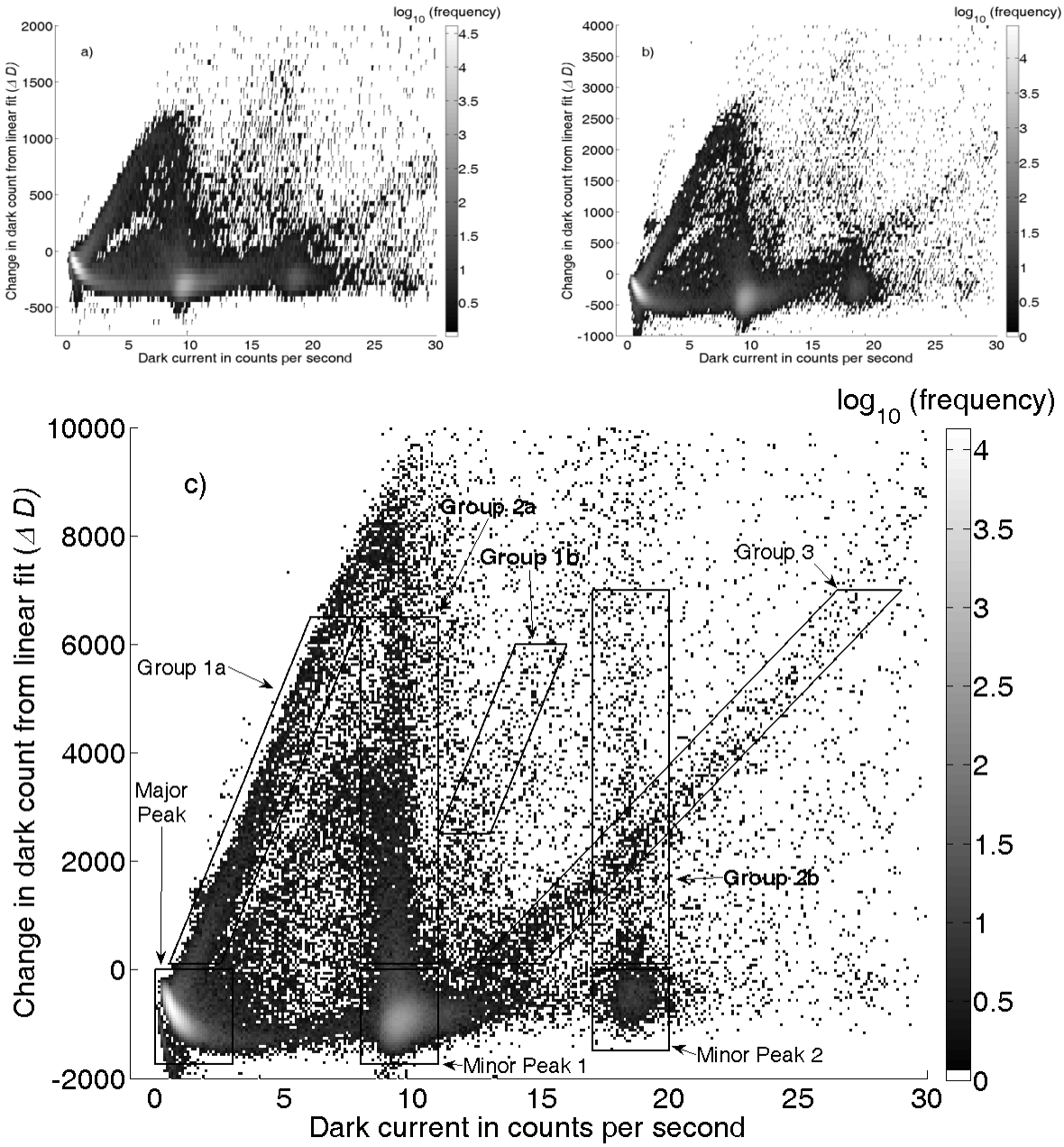

Fig. 4: Dark current from linear fit versus the change in dark count, ΔD, for the Meade Pictor 416XT at 278 K evaluated at (a) 640 s, (b) 900 s, (c) 1,800 s.

Fig. 5 illustrates the behavior of a typical pixel representing each group. Pixel 1a, 1b, 2a, 2b, and 3 all belong to their respective group name, and as one would expect, pixels from these groups show various degrees of nonlinearity in the dark current with long exposure times. Pixel 6, a hot pixel located in Minor Peak 1, is shown to have a large, mostly linear, dark current in Fig. 5a. Pixel 5 is located in Minor Peak 2 and has an even larger increase in dark count. Pixel 4 is a typical example of a regular pixel located in the Major Peak.

Grouping	Approximate Pixel Count (393,216 total pixels)
Major Peak	324,000
Minor Peak 1	36,000
Minor Peak 2	1,700
Group 1a	4,000
Group 2a	6,000
Group 1b	400
Group 2b	1,500
Group 3	1,300

Table 2 -Pixel count of groups, as shown in Fig. 4(c), for the Meade Pictor at an exposure time of 1,800s

From Fig. 5a it appears that pixels have either a linear time dependence of the dark count (pixels in the three peaks) or a negative curvature (other pixels). However, a closer examination of the short exposure times, as shown in Fig. 5b, reveals that all pixels initially have a positive curvature. This positive curvature explains why fits done at short exposure times to obtain Fig. 4 result in a negative baseline for ΔD where the three peaks are located. The initial smaller slopes at low exposure times will cause the extrapolated fits to predict smaller dark count values for all pixels if it would not be for the later occurring negative curvatures for some pixels.

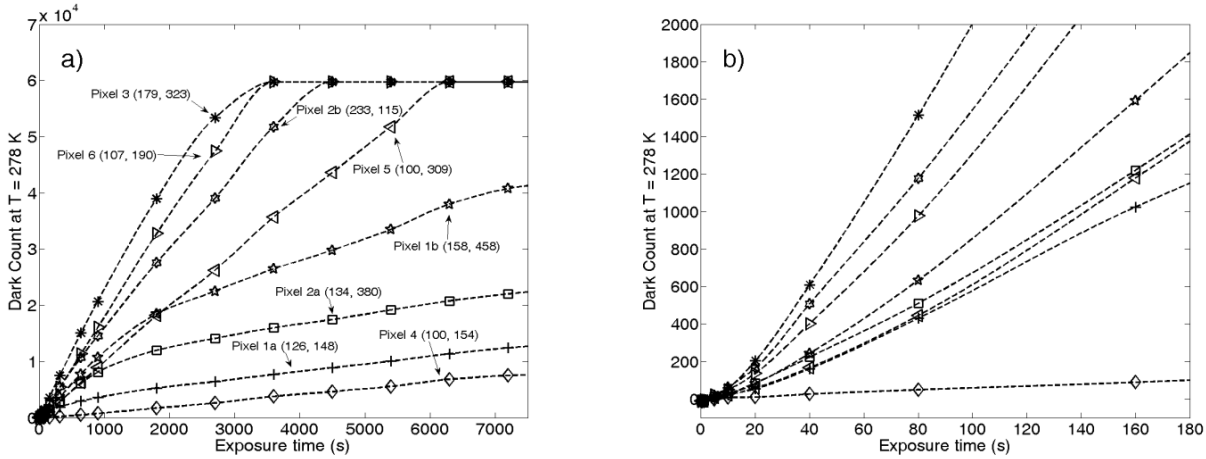

Fig. 5: Dark count at 278K as a function of exposure time for eight pixels for the Meade Pictor 416XT. (a) Exposure times up to 7,200 s. (b) Enlargement with exposure times up to 180 s.

3. DISCUSSION

Dark current is the thermally assisted excitation of electrons from the valence into the conduction band. From the dark current distribution of an individual dark frame one can find two distinct peaks for the SBIG camera and three peaks for the Meade camera. The first peak contains the majority of pixels for each camera. These pixels are devoid of any midgap impurity that causes the high dark current of hot pixels. The KAF-1602E chip in the SBIG camera appears to have one type of impurity which causes a number of pixels (1.1%) to become hot (Minor Peak). The KAF-0400 sensor has a larger fraction of hot pixels with 9.1% located in the Minor Peak 1. The larger number of impurities increases the likelihood of finding two impurities in the same pixel possibly giving rise to a smaller, but distinct, second peak (Minor Peak 2). One would expect that an impurity produces dark current at the same rate, filling a pixel's well and causing a linear pixel count until full well is reached. However, the data presented above clearly shows that this is not true for all pixels. With increasing exposure time, pixels in Group 2 stop being hot and start to behave more like pixels without midgap impurities. In a sense, the impurity that is present becomes inactive. To explain this phenomenon we need to look in more detail at the design of a CCD sensor.

Electrons excited into the conduction band either by photons or through thermal energy are actively collected only within the potential well. Front-illuminated imagers generally have a large field free region where electrons are not actively collected. Free electrons generated in the field-free part of the imager have to diffuse first toward the potential well before being collected and counted. Depending on the life time, some electrons will recombine with a hole before collection or diffuse into adjacent pixels. Hence, electrons generated at impurity sites outside the potential well will not contribute to the dark count in the same amount as electrons that are generated by an impurity in the well. The edge of the potential well is not static throughout the exposure. The depletion edge moves closer to the front surface with increasing number of electrons collected in the well. Impurities located close to the depletion edge can therefore move from being within the well at the beginning of the exposure to being in the field-free region at the end of the exposure. Since the collection efficiency of electrons generated outside the well is lower than the efficiency within the well, the rate at which these impurities generate dark current decreases with increasing exposure time. This phenomenon can explain the negative curvature of several pixels in Figs. 2 and 5. Figures 3 and 4 could therefore be used to get information on an impurity's location. Major Peak pixels are devoid of any midgap impurity generating an intrinsic low dark count. Minor Peak pixels contain one impurity causing an increase in dark current. The impurity is located well within the depletion region and therefore generates dark current at a constant rate until the pixel reaches saturation. Hot pixels, including Minor Peak 1 pixels are randomly distributed across the chip. Assuming a random distribution of impurities that cause a pixel to become hot, it would be expected that some pixels have two impurities. Two hot impurities can give rise to the pixels located in Minor Peak 2 for the Meade camera. Due to the smaller number of Minor Peak pixels in the SBIG camera, having two impurities in one pixel is less likely and a second peak is barely, or arguably not, visible in Fig. 3. We hypothesize that Group 1 and Group 2 pixels have impurities close to the depletion edge. The lower the dark current (x-axis in Fig. 3 and 4) as obtained from the low exposure time fits, the faster the impurity moves outside the depletion region. Hence, Group 1 pixels, with an impurity very close to the initial depletion edge, have different dark current values even for low exposure times. The dark current for all Group 1 pixels decreases such that the longer exposure times (such as at 640 s, 900 s and 1,800 s in Figs. 3 and 4) yield a smaller dark count than expected from the linear fit. The behavior of Group 2 pixels is similar. Again, for the long exposure times the dark current decreases because the impurity has moved out of the depletion region. At the short exposure times used for the fit, the impurity is still within the well and the dark current is therefore the same as for Minor Peak pixels. The same explanation can be applied to Group 1a and Group 2a pixels in the KAF-0400 sensor. Due to the larger number of impurities one also finds pixels with one impurity within the depleted well and one impurity at the initial depletion edge resulting in Group 1b and Group 2b. The occurrence of Groups 3 in both chips is believed to be the result of further distinction within the peaks themselves but is not well understood at this point. The global positive curvature for the Meade camera at short exposure times must be specific to the chip design of the KAF-0400 sensor which results in a pathway for thermally generated electrons to slowly activate with short exposure times. More work needs to be done to explain this phenomenon.

If filling the potential well with thermally excited electrons causes the depletion region to shrink and to move some impurities out of the well, the same should happen if one fills the well with photoelectrons. We found that this is indeed the case.[12] Fig. 6 shows the change in dark current after an imager was exposed to an initial brief flash of light. Fig. 6 was generated in a similar manner as Figs. 3 and 4. Here the x-axes show the dark count in a 600 s dark frame and the y-axes show the difference between the dark count of a regular dark frame and a frame that has been illuminated with light. For example, one would expect that a Group 1 pixel would produce very little dark current if the well was filled with photoelectrons causing the impurity to sit outside the depletion edge. This is found to be true; for example, Pixel 1 for the SBIG camera has a dark count of 1,589 counts at the 600 s dark frame, but only a dark count of 239 counts if illuminated with light (approximately 26,000 counts as is shown in Fig. 6). The resulting change in dark count is therefore almost as large as the dark count resulting in a pixel with D_{600}=1,589 and ΔD_{Light}=1,349. Hence, the initial flash of light suppresses the dark current almost entirely. Group 1 pixels are therefore located along a line where ΔD_{Light} is almost as large as D_{600}. More generally, it is apparent from Fig. 6 that the identified groups occur for both cameras for the light exposure analysis as well. Furthermore, evolution of the groups appears to be similar with increasing full wells as is shown in the progression of increasing exposure times in Figs. 3 and 4 as well as with increasing light flash as seen in Fig. 6.

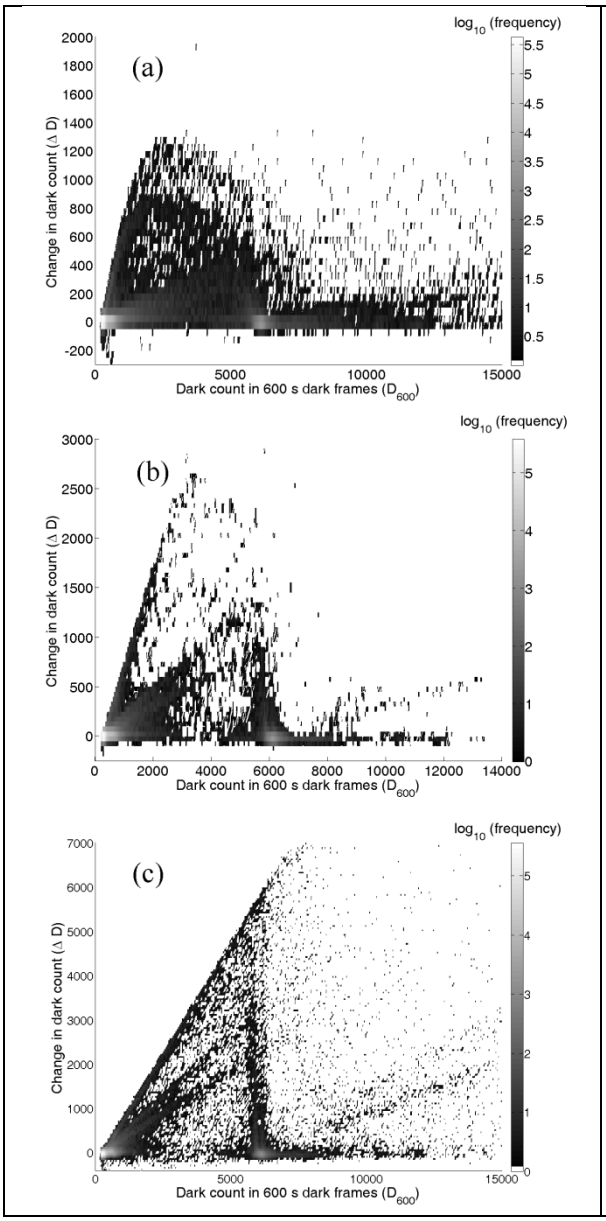

Fig. 6: Change of dark count after illumination versus dark count of a 600 s dark frame for the SBIG ST-8XE at 288K.[12] Average initial count due to the light exposure of approximately (a)2,500 (b) 8,500, and (c)26,000.

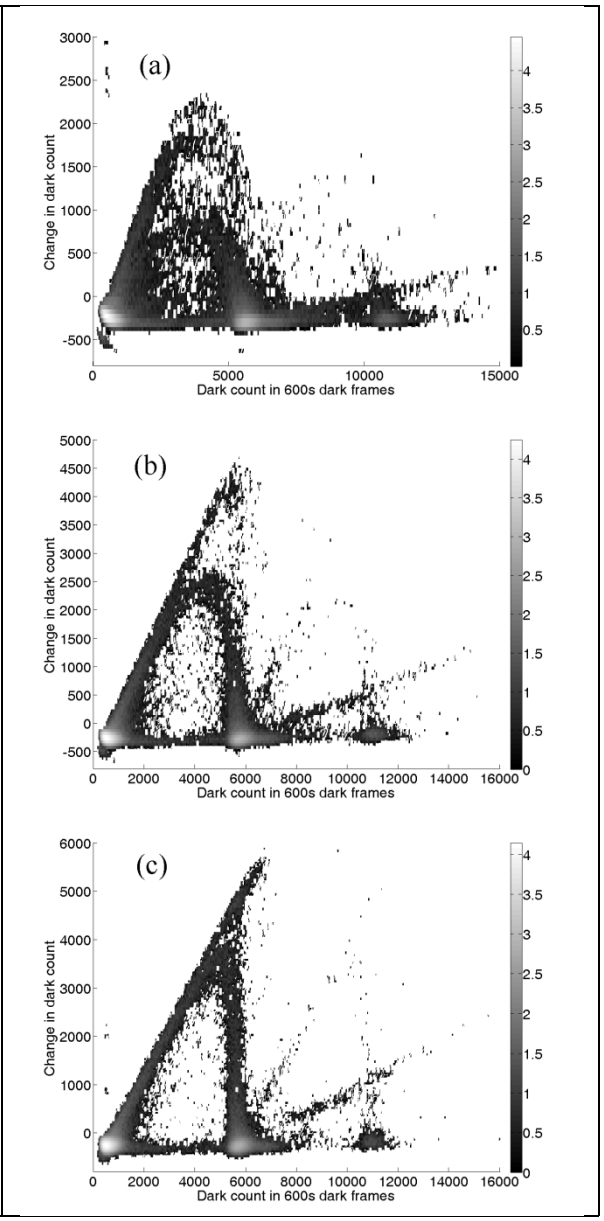

Fig. 7 *Change of dark count after illumination versus dark count of a 600 s dark frame for the Mead Pictor 416XT at 278K.[12] Average initial count due to the light exposure of approximately (a)12,500, (b)25,500, and (c)42,100.*

4. CONCLUSION

Previous work on dark current in digital imagers has focused on its temperature dependence. Using temperature data one can, for example, find the activation energy characteristic of a particular type of impurity. We found that the nonlinear time dependence of dark current can point to an impurity's location. An impurity located near the depletion edge will not produce a dark count at a steady rate. Scaling the dark count of pixels with such impurities is therefore problematic. Since the dark current depends on the number of already collected electrons, dark count correction becomes especially complicated if one considers that during an exposure, electrons are generated thermally as well as through

photoexcitation. Our study shows that accurately predicting the dark count of certain pixels necessitates knowing how the depletion edge moved during a particular exposure.

ACKNOWLEDGEMENTS

The authors would like to acknowledge financial support by Portland State University's "Faculty Development Grant" and the MJ Murdock charitable trust's "Partners in Science" program. Thank you to Tammy Johnson for collecting data for this research.

REFERENCES

[1] McGraph, R. D., Doty, J., Lupino, G., Ricker, G. and Vallerga, J. . "Counting of deep-level traps using a charge-coupled device," IEEE Trans. Electron Devices, vol. ED- **34**, no. 12, 2555-2557 (1987)
[2] McColgin, W. C., Lavine, J. P., Kyan, J., Nichols, D. N., and Stancampiano, C. V. . "Dark current quantization in CCD image sensors," IEDM Tech. Dig., 113–116. (1992)
[3] McColgin, W. C., Lavine, J. P., and Stancampiano, C. V. . "Probing metal defects in CCD image sensors," Mater. Res. Soc. Symp. Proc. **378**, 713, 1995
[4] McColgin, W. C., Lavine, J. P., and Stancampiano, C. V., and Russell, J. B. . "Deep-level traps in CCD image sensors," Mater. Res. Soc. Symp. Proc., **510**, 475, (1998)
[5] Widenhorn, R., Blouke, M. M, Weber, A., Rest, A., and Bodegom, E., "Temperature dependence of dark current in a CCD", Proc. SPIE Int. Soc. Opt. Eng. **4669**, 193 (2002)
[6] Grove, A. S. , [Physics and Technology of Semiconductor Devices], John Wiley & Sons, Hoboken, NJ, (1967)
[7] Sah, C. T., Noyce, R. N., and Shockley, W., "Carrier Generation and Recombination in p-n Junction and p-n Junction Characteristics," Proc. IRE **45**, 1228, (1957)
[8] Hall, R. N. . "Electron-Hole Recombination in Germanium," Phys. Rev. **87**, 387, (1952)
[9] Shockley, W. and Read, W. T. . "Statistics of the Recombination of Holes and Electrons," Phys. Rev. **87**, 835, (1952)
[10] Sze, S.M., [Physics of Semiconductor Devices], 2nd ed., John Wiley & Sons, Hoboken, NJ, (1981)
[11] Widenhorn, R., Rest; A., Blouke; M.M., Berry; R. L., Bodegom, E., "Computation of dark frames in digital imagers," Proc. SPIE 6501, 650 103 (2007)
[12] Widenhorn, R., Hartwig, I., Dunlap, J. C., and Bodegom, E., "Measurements of dark current in a CCD imager during light exposures," Proc. SPIE 6816, 681 60B (2008)